AIMS Energy, 11(4): 683–693.
DOI: 10.3934/energy.2023034
Received: 20 April 2023
Revised: 19 June 2023
Accepted: 09 July 2023
Published: 28 August 2023

http://www.aimspress.com/journal/energy

Research article

Numerical study and optimization of GO/ZnO based perovskite solar cell using SCAPS

Norsakinah Johrin[1], Fuei Pien Chee[1,*], Syafiqa Nasir[1] and Pak Yan Moh[2,3,*]

[1] Physics with Electronic Programme, Faculty of Science and Natural Resources, Universiti Malaysia Sabah
[2] Industrial Chemistry Programme, Faculty of Science and Natural Resources, Universiti Malaysia Sabah
[3] Water Research Unit, Faculty of Science and Natural Resources, Universiti Malaysia Sabah

* **Correspondence:** Email: fpchee06@ums.edu.my, pymoh@ums.edu.my; Tel: +60168607582.

Abstract: This paper focuses on the numerical study of hybrid organic-inorganic perovskite solar cells. It investigates the incorporation of a graphene oxide (GO) thin layer to enhance solar cell efficiency. The study demonstrates that the GO layer improves interaction with the absorber layer and enhances hole transportation, resulting in reduced recombination and diffusion losses at the absorber and hole transport layer (HTL) interface. The increased energy level of the Lower Unoccupied Molecular Orbital (LUMO) in GO acts as an excellent electron-blocking layer, thereby improving the V_{OC}. The objective is to explore different structures of perovskite solar cells to enhance their performance. The simulated solar cell comprises a GO/$FASnI_3$/TiO_2/ZnO/ITO sandwich structure, with $FASnI_3$ and ZnO thicknesses adjusted to improve conversion efficiency. The impact of thickness on device performance, specifically the absorber and electron transport layers, is investigated. The fill factor (FF) changes as the absorber and electron transport layers (ETL) increase. The FF is an important parameter that determines PSC performance since it measures how effectively power is transferred from the cell to an external circuit. The optimized solar cell achieves a short-circuit current density (J_{SC}) of 27.27 mA/cm^2, an open-circuit voltage (V_{OC}) of 2.76 V, a fill factor (FF) of 27.05% and the highest power conversion efficiency (PCE) of 20.39% with 400 nm of $FASnI_3$ and 300 nm of ZnO. These findings suggest promising directions for the development of more effective GO-based perovskite solar cells.

Keywords: solar cell; graphene oxide; perovskite; fill factor; power conversion efficiency; SCAPS

1. Introduction

The great potential of PSCs is demonstrated by the fact that these cells' efficiency increased within a decade and has continued to increase to this century [1]. Third-generation perovskite solar cells, a novel topic for solar energy research, are currently the focus of interest in the scientific community among the various types of solar cells since they can be implemented at a cheap cost with high efficiency [2]. Graphene oxide (GO) has grown in prominence in recent years for its useful application in solar energy because of its excellent electrical, mechanical, thermal and optical properties [3]. By including graphene in the device's structure, the field of hybrid organic-inorganic devices has developed, making them more effective [4]. The FF of the solar cell and the efficiency of power conversion are improved by increasing the GO carrier density. Device performance is greater with a higher GO carrier density than a low one [5,6]. Due to its possible electrical and optical properties, GO is used as an HTL. Due to the improved charge transport properties of graphene oxide and increased contact with the absorber layer, a J_{SC} and PCE rose dramatically with increasing HTL layer thickness [3]. During real operation, the rate of heat dissipation from the graphene layer to the environment accelerates, boosting the cell's thermal stability. The cell achieved an efficiency of 9.12%, and its critical parameters—doping density and GO layer gap—can be readily improved to increase efficiency [4].

ZnO absorbs photons in the UVC region at around 300 nm and has a bandgap of 3.3 eV. A tiny coating of ZnO may induce leakage current, whereas a thick layer may result in a low carrier separation rate [7]. ZnO has been identified as a viable material in solar cell applications due to its comparatively high conductivity, electron mobility, photo-corrosion resistance and inexpensive cost [8]. ZnO materials have physical qualities similar to TiO_2 but substantially better electron mobility. Furthermore, there are numerous easy techniques for fabricating ZnO nanoparticles with minimal cost and energy consumption [9]. Amal Bouich et al. propose that the bandgap of their absorber layer makes PSC the most responsive to changes in thickness. SCAPS-1D software simulated the model and examined how the antisolvent affected its performance. According to reports, toluene treatment of the $MASnI_3$ films shows V_{oc}, J_{sc}, FF and Eta as 0.90 V, 13.69 mA/cm^2, 84.01% and 10.44% [10]. After optimization, the simulated model of the solar cell structure, which is CZTS/PSC/CZTS/CdS/ZnO/FTO, achieved a 25.95% efficiency gain. The performance of photovoltaic devices is critically dependent on the absorber layer and its thickness variation. At each different thickness, there was a significant impact on the solar cell J-V characteristics curve. The absorber layer's thickness was increased, creating a greater capacity to capture solar photons [11]. $FASnI_3$, a Pb-free halide perovskite formamidinium tin iodide, has received a lot of interest. These findings show that the key research challenges for high performance $FASnI_3$ based perovskite solar cell (PSCs) are to optimize the interface property and band offset, improve Sn^{2+} stability and reduce absorber layer defect density [12]. One of the toxic-free, very stable perovskite materials that has gained notice recently and has been used as an absorber layer in several solar cell systems is formamidinium tin iodide. Modeling and simulations have been done for the double-absorber solar cell using $FASnI_3$ and C_2N as echo-friendly absorber materials, as noted by S. Yasin et al. [13]. Other $FASnI_3$ values include conduction band and valence band effective density of states (EDOS) of 1×10^{18} cm^{-3} and electron and hole thermal velocities of 10^{17} cm/s for all layers [14].

By setting up a demonstration example in Solar Cell Capacitance Simulator (SCAPS), advanced electrical modeling of copper indium gallium diselenide solar cells is demonstrated (Solar Cell Capacitance Simulator). Because of the sensitivity of such barriers to the beginning state and operating voltage, the current-voltage properties, notably the fill factor, may be considerably reliant on the initial

circumstances [15]. According to a paper by Ghazi Aman Nowsherwan et al, the greatest efficiency of an improved organic solar cell is reported to be 17.36% following cell enhancement. The PTB_7:$PC_{71}BM$ has a PCE of 10.07% when utilized as an absorber layer with graphene oxide HTL. J_{SC} and PCE rose dramatically when the thickness of the HTM layer was increased due to the improved charge transport properties of GO and increased contact with the absorber layer [3]. The $FASnI_3$ layer impact on the GO/ZnO interface has been explored in this context to analyze the J_{SC} V_{OC}, FF and PCE. This study explores the impact of the thickness of the absorber and ETL on GO in PSCs. The main objective of this research is to optimize the parameters of PSCs to achieve a higher PCE and lower manufacturing cost.

2. Methodology

A SCAPS-1D numerical simulation was used to calculate V_{OC}, FF, J_{SC} and efficiency. This simulator's operational temperature, thickness, voltage, frequency, light and quantum efficiency parameters are promising. Figure 1 depicts the simulator settings and device layout for the GO/ZnO solar cell. This program can generate a band diagram, an electric field, carrier densities and partial carrier recombination. Front indium tin oxide (ITO) on glass substrate is employed in the design. P-type GO emitter contact is kept constant throughout all simulations, and ZnO thicknesses range from 300 to 500 nm, whereas $FASnI_3$ thicknesses range from 200 nm to 400 nm. According to Tingting Shi et al., a maximum PCE of 9.75% could be reached with an absorber thickness of 300 nm. Since it is closely related to the recombination, transmission and collection of photogenerated carriers, the thickness of the absorber is important characteristic for solar cell performance. The dominant donor and acceptor in $FASnI_3$ perovskite are FA interstitial (FAi) and VSn, respectively, and their relative concentrations are highly dependent on the growth circumstances [16].

The photovoltaic properties of hybrid solar cells were experimentally evaluated and compared. It was reported by Sakshi Tyagi et al. that a simulated analysis of the different characteristics of graphene-contact ZnO hybrid solar systems where a graphene layer on top that functions as a hole transport layer. Simulated V_{OC}, J_{SC}, FF and PCE values for ZnO/GO are 0.79 V, 12.46 mA/cm^2, 52.14% and 8.46%, respectively [4]. In this research, the impact of GO as the HTL on the electrical performance of the perovskite solar cell with the structured GO/$FASnI_3$/TiO_2/ZnO were investigated using the SCAPS-1D programme. Simulated V_{OC}, J_{SC}, FF and PCE values are 2.78 V, 26.67 mA/cm^2, 27.04% and 20.05%, respectively.

Solar cells using a hole transport layer-less design and ZnO as an electron selective contact in free air achieved an efficiency of 3.02%. It showed that low resistivity electron selective connections in the ZnO matrix are achievable, which is critical for improving performance. It was able to achieve a maximum efficiency of 4.52%: composite GO using our final ZnO devices [17]. Table 1 displays the simulation results for the PV parameters under sun. $FASnI_3$ (1.41 eV) has lower energy bandgaps in tin-based perovskite solar cells than $MAPbI_3$ (1.59 eV), which can increase photon absorption from sunshine [18,19]. Higher charge transfer is provided by the two-dimensional GO network in the matrix, which improves electron acquisition and lowers interfacial resistance. Reducing the device's overall series resistance also has an impact on the FF. The space charge area at the interface is impacted by higher electron mobilities and improved charge collection, which improves device performance [17]. Until recently, the J_{SC} of Sn^- based perovskite solar cells have nearly reached their maximum. The biggest impediment to increasing efficiency is their poor V_{OC}, which is caused by significant charge recombination and mismatched band alignment at the interfaces [20]. There are certain limitations in

the SCAPS-1D, which are the number and type of panels that can be opened or operated at the same time. This accuracy is frequently insufficient for the simulation of semiconductors, and caution should be taken to prevent numerically unstable operations [21].

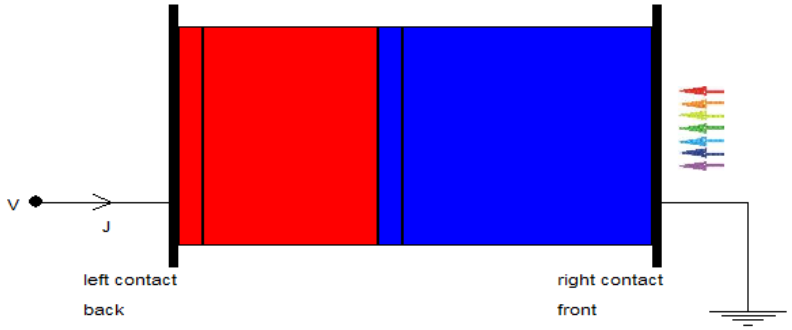

(a)

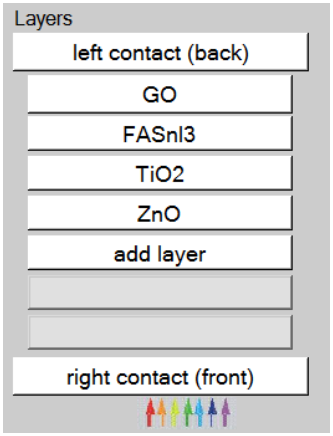

(b)

Figure 1. SCAPS Layout (a) and model (b) for emerging solar cell.

Table 1. Basic parameter of each layer of the device [3–5,7,12–14,22–30].

Materials Parameters	HTL GO	Absorber layer $FASnI_3$	Passivation layer TiO_2	ETL ZnO
Thickness 't' (nm)	50	350	50	500 (varied)
Band gap 'E_g' (eV)	2.48	1.36	2.26	3.2
Electron affinity 'λ' (eV)	3.4	4.12	4.20	4.210
Dielectric permitivity 'εr'	10	8.2	10	9
CB effective density of states 'N_C' (cm^{-3})	1.8×10^{19}	1.0×10^{18}	2.0×10^{17}	2.2×10^{18}
VB effective density of states 'N_V' (cm^{-3})	2.2×10^{18}	1.0×10^{18}	6.0×10^{17}	1.8×10^{19}
Electron mobility 'μ_n' (cm^2/V.s)	2.0×10^{5}	22	1.0×10^{2}	6×10^{1}
Hole mobility 'μ_p' (cm^2/V.s)	1.23×10^{2}	22	25	1×10^{1}
Shallow donor density (N_D) (cm^{-3})	0	0	1.0×10^{17}	1×10^{19}
Shallow acceptor density (N_A) (cm^{-3})	1×10^{18}	7×10^{16}	0	0

3. Results and discussion

The SCAPS simulation shows variations in absorber and ETL layer thickness effect PV performance. The absorber layer and ETL thickness values were adjusted for various device features of the layers in each segment to examine the real effects of altering the thickness of the perovskite layer on efficiency. The impacts of layer absorber and ETL were studied. Figure 2 shows the current density vs. voltage curve (J-V curve). The J-V curve of a solar cell under direct sunlight (AM 1.5 G, 100 mW/cm^2) may be utilized to calculate PCE. The voltage is applied while the current is measured with a load resistor. The open-circuit voltage and short-circuit current density are represented as V_{OC} and J_{SC}, respectively. The greater fill factor (FF) is caused by lower series resistance (R_S) and higher shunt resistance (R_{sh}). When the V_{OC}, J_{SC} and FF from the J-V curve are obtained, the PCE can be calculated. The J_{SC} and the light-generated current are the same for a perfect solar cell with most moderate resistive loss mechanisms. The V_{OC} is proportional to the amount of forward bias on the solar cell caused by the solar cell junction's bias with the light-generated current. PCE is the difference in power between the externally applied voltage and the energy of the emitted photons, which usually includes voltage drops across the internal resistance. The value of J_{SC} in this structure is 26.67 mA/cm^2, V_{OC} is 2.78 V, FF is 27.04% and PCE is 20.05%.

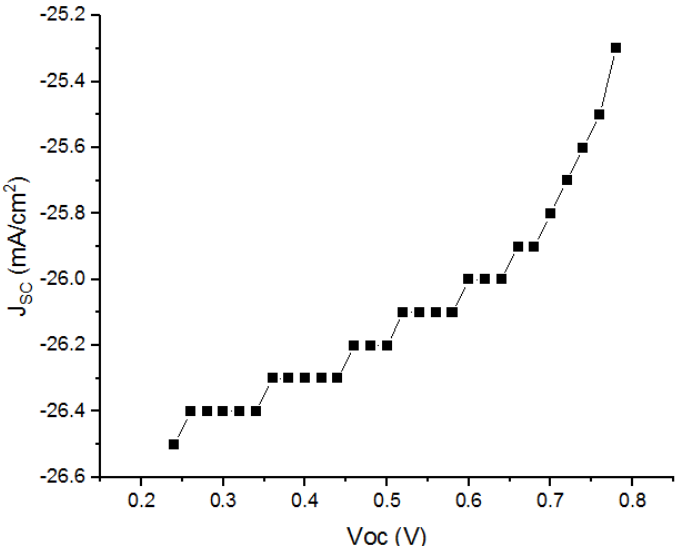

Figure 2. The current density Vs. Voltage Curve (J-V curve) of GO/$FASnI_3$/TiO_2/ZnO.

3.1. Effects of the perovskite absorber layer and Electron Transport Layer (ETL) thickness on device performance

Changing this value in specific layers has an effect on efficiency. The effect of thickness modifications is seen in Figure 3. When demonstrated in Figure 3a–d, as the thickness of the absorber layer grows (200–400 nm), all parameters except the fill factor increase. This reveals that the V_{OC}, J_{SC} and PCE values are rising from 2.468–2.551 V, 22.515–27.505 mA/cm^2 and 17.23%–20.54%, while the FF values are dropping from 31%–29.27%. In the 200 nm region, the greatest fill factor is recorded. According to these figures, the best thickness for this layer is 400 nm. FF represents the ability to

transmit the complete available power to the created electrical load [3]. Changing the thickness of the HTL has no effect on performance measures and is not depicted in the image [31].

Modifying the thickness of the ZnO layer has an impact on the performance of the device, as shown in Figure 3e–h. All metrics, except the fill factor, decrease as ETL thickness changes (300–500 nm). The value of FF grew significantly as well, although this can be ignored. This is likely due to the consistent generation of charge carriers in the lead-free perovskite material, while the significant fall in PCE values could be related to increased charge recombination at the ETL/Absorber interface [14]. The V_{OC}, J_{SC}, FF and PCE values are 2.58–2.57 V, 27.07–26.94 mA/cm^2, 29.17%–29.25% and 20.34%–20.24%, respectively. Based on these results, the optimal thickness for the ZnO layer is 300 nm.

The FF is an important metric for evaluating the performance of PSCs, as it measures the efficiency of power transfer from the cell to an external circuit. However, FF is often reduced by carrier recombination, which affects carrier lifespan and hence the amount of current extracted from the device [32]. As a result, carrier mobility and longevity are also goal criteria to improve in order to boost PSC fill factors [33]. The FF increases modestly at low intensities and subsequently declines as the intensity of the irradiation increases [34,35]. The decrease in FF is primarily due to internal recombination within the lead-free perovskite material, which is caused by the short lifetime of electron (t_n) and hole (t_p) charge carriers, which does not allow adequate time for charge carriers to develop conduction band at lead-free perovskite material [14].

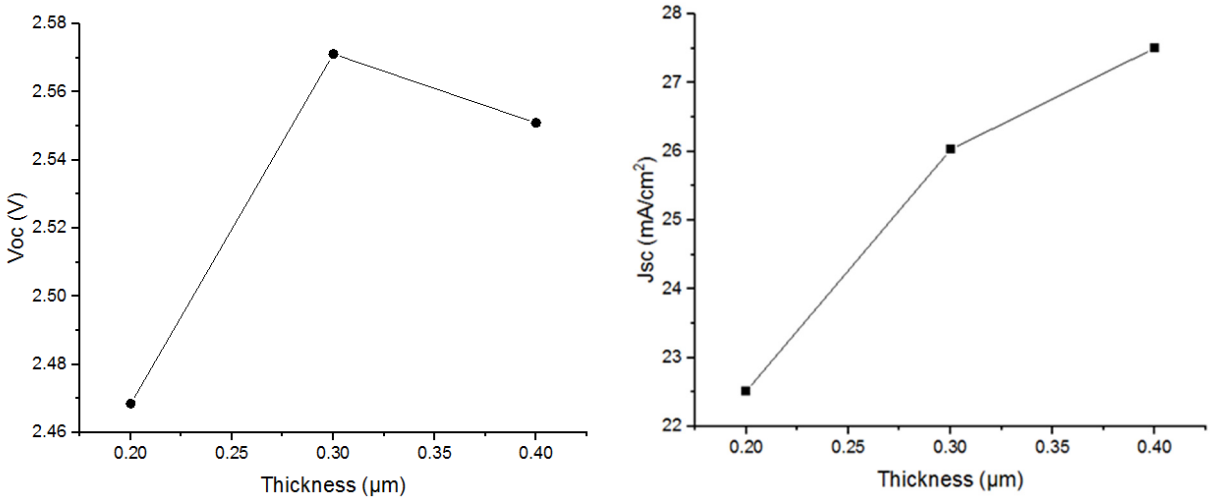

(a) (b)

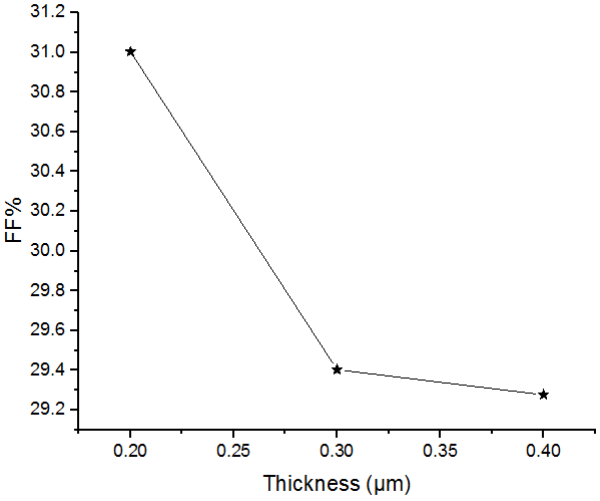
FF%
Thickness (μm)

(c)

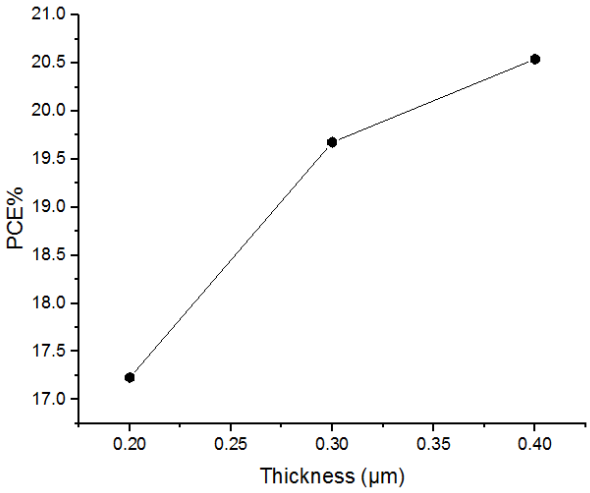
PCE%
Thickness (μm)

(d)

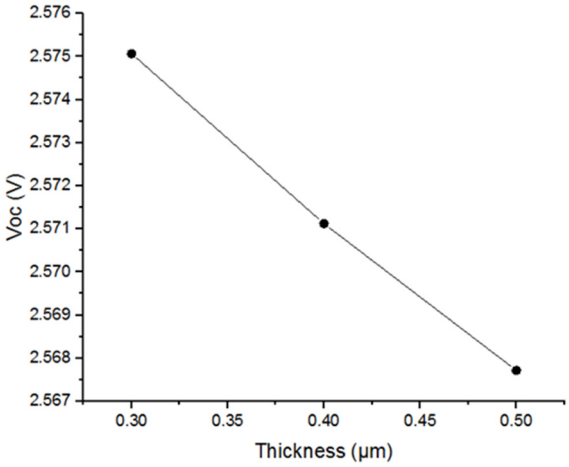
Voc (V)
Thickness (μm)

(e)

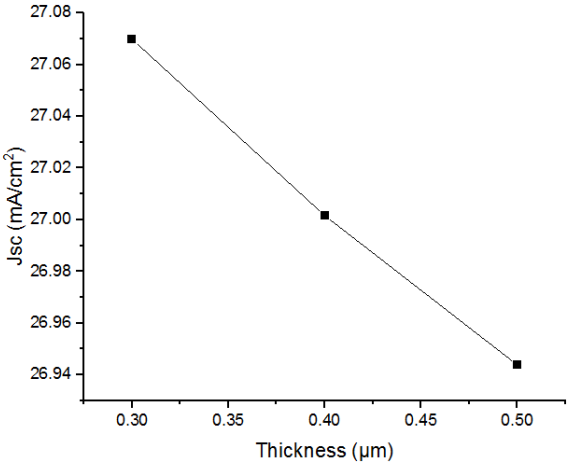
Jsc (mA/cm2)
Thickness (μm)

(f)

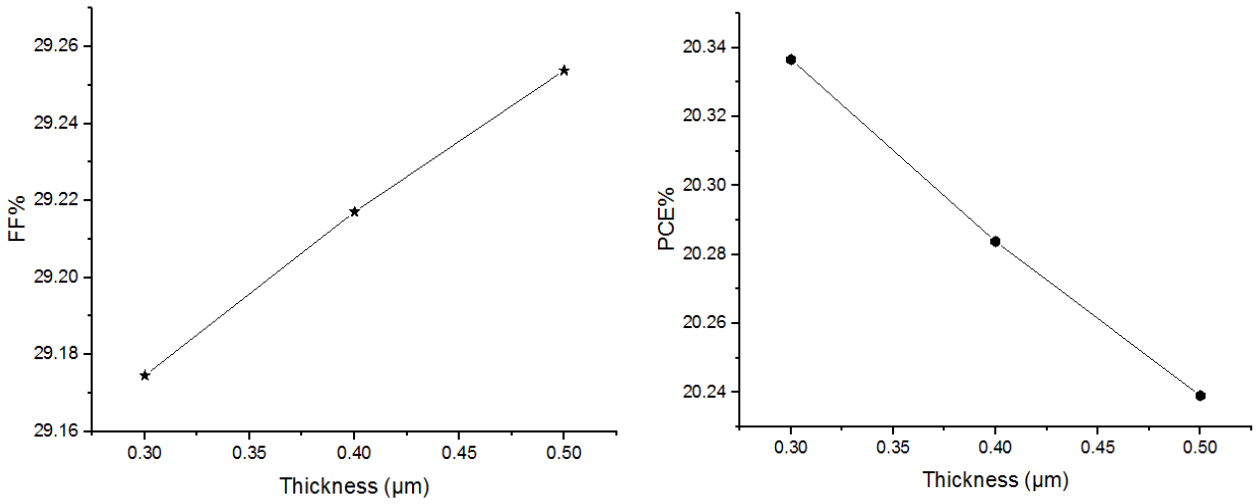

(g) (h)

Figure 3. (a–d) Variations in absorber thickness as a function of performance parameters (keeping the fix ETL and HTL thickness), and (e–h) ETL thickness as a function of the performance parameters.

4. Conclusions

In this paper, the impact of GO as HTL on the electrical performance of the perovskite solar cell with the structure is investigated using SCAPS-1D. GO/$FASnI_3$/TiO_2/ZnO/ITO were optimized by investigating the influence of absorber and ETL layer thicknesses on power conversion efficiency. Electron transport and absorber layers increase, causing fill factor (FF) modifications. The FF quantifies the effectiveness of power transfer from the cell to an external circuit, making it a crucial parameter to determine PSC performance. After optimizing the fundamental parameters, the final performance characteristics for JSC, VOC, FF and PCE of the solar cell device obtained increased to 27.27 mA/cm2, 2.76 V, 27.05% and 20.39% and the optimal thicknesses were discovered to be 400 nm and 300 nm, respectively, with a higher power conversion efficiency. To show that PSC device performance can be enhanced by modifying the device parameters in the future, a design of a PSC with a high efficiency of 20.39% is presented along with the simulated results. The results will provide better predictions for thin-film solar cells based on lead-free perovskite solar cells. The development of enhanced numerical models of solar cell performance plays a crucial role. Thus, this numerical model can be used to predict alternative solar cell based devices for improved solar cell conversion efficiency.

Use of AI tools declaration

The author declare that the research was conducted and presented in this article have not used AI tools at all stages of the research process.

Conflict of interest

The authors declare no conflict of interest.

Acknowledgment

This work is supported by Ministry of Higher Education Fundamental Research Grant Scheme (FRGS) Year 2020, FRGS/1/2020/STG07/UMS/02/1 titled "Explication on the Damage Mechanism Induced by High Energy Radiation on ZnO based Photoconductive Radiation Detector for Space Borne Application" and GUG0579-1/2023 titled "Enhancement of Graphene based Perovskite Solar Cell using Electron Beam Radiation".

References

1. Roy P, Kumar SN, Tiwari S, et al. (2020) A review on perovskite solar cells: Evolution of architecture, fabrication techniques, commercialization issues and status. *Sol Energy* 198: 665–688. https://doi.org/10.1016/j.solener.2020.01.080
2. Izadi F, Ghobadi A, Gharaati A, et al. (2021) Effect of interface defects on high efficient perovskite solar cells. *Optik* 227: 166061. https://doi.org/10.1016/j.ijleo.2020.166061
3. Nowsherwan GA, Samad A, Iqbal MA, et al. (2022) Performance analysis and optimization of a PBDB-T: ITIC based organic solar cell using graphene oxide as the hole transport layer. *Nanomater* 12. https://doi.org/10.3390/nano12101767
4. Tyagi S, Singh PK, Tiwari AK (2022) Photovoltaic parameter extraction and optimisation of ZnO/GO based hybrid solar trigeneration system using SCAPS 1D. *Energy Sustainable Dev* 70: 205–224. https://doi.org/10.1016/j.esd.2022.08.001
5. Touafek N, Mahamdi R, Dridi C, et al. (2021) Boosting the performance of planar inverted perovskite solar cells employing graphene oxide as HTL. *Dig J Nanomater Bios* 16: 705–712. Available from: https://chalcogen.ro/705_TouafekN.pdf.
6. Nguang SY, Liew ASY, Chin WC, et al. (2022) Effect of graphene oxide on the energy level alignment and photocatalytic performance of Engelhard Titanosilicate-10. *Mater Chem Phys* 275: 125198. https://doi.org/10.1016/j.matchemphys.2021.125198
7. Zyoud SH, Zyoud AH, Ahmed NM, et al. (2021) Numerical modeling of high conversion efficiency FTO/ZnO/CdS/CZTS/MO thin filmbased solar cells: Using Scaps-1D software. *Crystals* 11: 1468. https://doi.org/10.3390/cryst11121468
8. Wibowo A, Marsudi MA, Amal MI (2020) ZnO nanostructured materials for emerging solar cell applications. *RSC Adv* 10: 42838–42859. https://doi.org/10.1039/d0ra07689a
9. Zhang P, Wu J, Zhang T, et al. (2018) Perovskite solar cells with ZnO electron-transporting materials. *Adv Mater* 30: 1703737. https://doi.org/10.1002/adma.201703737
10. Bouich A, Marí-Guaita J, Soucase BM, et al. (2022) Manufacture of high-efficiency and stable lead-free solar cells through antisolvent quenching engineering. *Nanomater* 12: 2901. https://doi.org/10.3390/nano12172901
11. Shafi MA, Khan L, Ullah S, et al. (2022) Novel compositional engineering for ~26% efficient CZTS-perovskite tandem solar cell. *Optik* 253: 168568. https://doi.org/10.1016/j.ijleo.2022.168568

12. Li S, Liu P, Pan L, et al. (2019) The investigation of inverted p-i-n planar perovskite solar cells based on $FASnI_3$ films. *Sol Energy Mater Sol Cells* 199: 75–82. https://doi.org/10.1016/j.solmat.2019.04.023
13. Yasin S, Moustafa M, Al Zoubi T, et al. (2021) High efficiency performance of eco-friendly C_2N/$FASnI_3$ double-absorber solar cell probed by numerical analysis. *Opt Mater* 122. https://doi.org/10.1016/j.optmat.2021.111743
14. Kumar M, Raj A, Kumar A, et al. (2020) An optimized lead-free formamidinium Sn-based perovskite solar cell design for high power conversion efficiency by SCAPS simulation. *Opt Mater* 108: 110213. https://doi.org/10.1016/j.optmat.2020.110213
15. Burgelman M, Decock K, Khelifi S, et al. (2013) Advanced electrical simulation of thin film solar cells. *Thin Solid Films* 535: 296–301. https://doi.org/10.1016/j.tsf.2012.10.032
16. Shi T, Zhang HS, Meng W, et al. (2017) Effects of organic cations on the defect physics of tin halide perovskites. *J Mater Chem* 5: 15124–15129. https://doi.org/10.1039/C7TA02662E
17. Ahmed MI, Hussain Z, Mujahid M, et al. (2016) Low resistivity ZnO-GO electron transport layer based $CH_3NH_3PbI_3$ solar cells. *AIP Adv* 6: 065303. https://doi.org/10.1063/1.4953397
18. Kim MK, Jeon T, Park HI, et al. (2016) Effective control of crystal grain size in $CH_3NH_3PbI_3$ perovskite solar cells with a pseudohalide $Pb(SCN)_2$ additive. *CrystEngComm* 18: 6090–6095. https://doi.org/10.1039/c6ce00842a
19. Tao S, Schmidt I, Brocks G, et al. (2019) Absolute energy level positions in tin- and lead-based halide perovskites. *Nat Commun* 10: 2560. https://doi.org/10.1038/s41467-019-10468-7
20. Li S, Yang F, Chen M, et al. (2022) Additive engineering for improving the stability of tin-based perovskite ($FASnI_3$) solar cells. *Sol Energy* 243: 134–141. https://doi.org/10.1016/j.solener.2022.07.009
21. Burgelman M, Decock K, Niemegeers A, et al. (2016) SCAPS manual. *University of Ghent: Ghent, Belgium*. Available from: https://scaps.elis.ugent.be/SCAPS%20manual%20most%20recent.pdf.
22. Alipour H, Ghadimi A (2021) Optimization of lead-free perovskite solar cells in normal-structure with WO_3 and water-free PEDOT: PSS composite for hole transport layer by SCAPS-1D simulation. *Opt Mater* 120. https://doi.org/10.1016/j.optmat.2021.111432
23. Deepthi JK, Sebastian V (2021) Comprehensive device modelling and performance analysis of $MASnI_3$ based perovskite solar cells with diverse ETM, HTM and back metal contacts. *Sol Energy* 217: 40–48. https://doi.org/10.1016/j.solener.2021.01.058
24. Bello IT, Idisi DO, Suleman KO, et al. (2022) Thickness variation effects on the efficiency of simulated hybrid Cu_2ZnSnS_4-based solar cells using Scaps-1D. *Biointerface Res Appl Chem* 12: 7478–7487. https://doi.org/10.33263/BRIAC126.74787487
25. Tara A, Bharti V, Sharma S, et al. (2021) Device simulation of $FASnI_3$ based perovskite solar cell with $Zn(O_{0.3}, S_{0.7})$ as electron transport layer using SCAPS-1D. *Opt Mater* 119: 111362. https://doi.org/10.1016/j.optmat.2021.111362
26. Saeed F, Gelani HE (2022) Unravelling the effect of defect density, grain boundary and gradient doping in an efficient lead-free formamidinium perovskite solar cell. *Opt Mater* 124: 111952. https://doi.org/10.1016/j.optmat.2021.111952
27. Ait-Wahmane Y, Mouhib H, Ydir B, et al. (2021) Comparison study between ZnO and TiO_2 in CuO based solar cell using SCAPS-1D. *Mater Today: Proc* 52: 166–171. https://doi.org/10.1016/j.matpr.2021.11.535

28. Sawicka-Chudy P, Sibiński M, Wisz G, et al. (2018) Numerical analysis and optimization of Cu_2O/TiO_2, CuO/TiO_2, heterojunction solar cells using SCAPS. *J Phys Conf Ser* https://doi.org/10.1088/1742-6596/1033/1/012002
29. Mouchou RT, Jen TC, Laseinde OT, et al. (2021) Numerical simulation and optimization of p-NiO/n-TiO_2 solar cell system using SCAPS. *Mater Today: Proc* 38: 835–841. https://doi.org/10.1016/j.matpr.2020.04.880
30. Enebe G, Lukong V, Mouchou R, et al. (2022) Optimizing nanostructured TiO_2/Cu_2O pn heterojunction solar cells using SCAPS for fourth industrial revolution. *Mater Today: Proc* 62: S145–S150. https://doi.org/10.1016/j.matpr.2022.03.485
31. Ghosh BK, Nasir S, Chee FP, et al. (2022) Numerical study of nSi and nSiGe solar cells: Emerging microstructure nSiGe cell achieved the highest 8.55% efficiency. *Opt Mater* 129: 112539. https://doi.org/10.1016/j.optmat.2022.112539
32. Guo X, Zhou N, Lou SJ, et al. (2013) Polymer solar cells with enhanced fill factors. *Nat Photonics* 7: 825–833. https://doi.org/10.1038/nphoton.2013.207
33. Proctor CM, Kim C, Neher D, et al. (2013) Nongeminate recombination and charge transport limitations in diketopyrrolopyrrole-based solution-processed small molecule solar cells. *Adv Funct Mater* 23: 3584–3594. https://doi.org/10.1002/adfm.201202643
34. Ryu S, Noh JH, Jeon NJ (2014) Voltage output of efficient perovskite solar cells with high open-circuit voltage and fill factor. *Energy Environ Sci* 7: 2614–2618. https://doi.org/10.1039/c4ee00762j
35. Rasmidi R, Mivolil DS, Chee FP, et al. (2022) Structural and optical properties of TIPS pentacene thin film exposed to gamma radiation. *Mater Res* 25. https://doi.org/10.1590/1980-5373-MR-2022-0227

AIMS Press